

# Efficacy assessment of newly-designed and locally-produced filtering facemasks during the SARS-CoV-2 pandemic.

Bob Boogaard<sup>1\*</sup>, Ali Tas<sup>4</sup>, Joep Nijssen<sup>2</sup>, Freek Broeren<sup>2</sup>, John van der Dobbelsteen<sup>2</sup>, Vincent Verhoeven<sup>3</sup>, Jip Pluim<sup>3</sup>, Sing Dekker<sup>3</sup>, Eric Snijder<sup>4</sup>, Martijn van Hemert<sup>4</sup>, Sander Herfst<sup>1</sup>.

<sup>1</sup> Department of Virology, Erasmus University Medical Center, Dr. Molewaterplein 40, 3015 GD Rotterdam, The Netherlands

<sup>2</sup> Department of Precision and Microsystems Engineering, Department of Biomechanical Engineering, Delft University of Technology, 2628CN, Delft, The Netherlands

<sup>3</sup> Department of Medical Physics, Department of Infection Prevention, Reinier de Graaf Gasthuis, Reinier de Graafweg 5, 2625 AD, Delft, The Netherlands

<sup>4</sup> Department of Medical Microbiology, Leiden University Medical Center, Albinusdreef 2, 2333 ZA, Leiden, The Netherlands

\* corresponding author: [b.boogaard@erasmusmc.nl](mailto:b.boogaard@erasmusmc.nl)

## Abstract (142 words)

The SARS-CoV-2 pandemic resulted in shortages of production and test capacity of FFP2-respirators. Such facemasks are required to be worn by healthcare professionals when performing aerosol-generating procedures on COVID-19 patients. In response to the high demand and short supply, we designed three models of facemasks that are suitable for local production. As these facemasks should meet the requirements of an FFP2-certified facemask, the newly-designed facemasks were tested on the filtration efficiency of the filter material, inward leakage, and breathing resistance with custom-made experimental setups. In these tests, the locally-produced facemasks were benchmarked against a commercial FFP2 facemask. Furthermore, the protective capacity of the facemasks was tested for the first time with coronavirus-loaded aerosols under physiologically relevant conditions. This multidisciplinary effort resulted in the design and production of facemasks that meet the FFP2 requirements, and which can be mass-produced at local production facilities.

**Keywords:** coronavirus filtration efficiency, facemask, FFP2, NaCl particle filtration, respirator.

## 37 INTRODUCTION

38

39 The severe acute respiratory syndrome coronavirus-2 (SARS-CoV-2) is a novel  
40 coronavirus that was first identified in December 2019 in Wuhan, China, in patients suffering  
41 from acute respiratory syndrome (2019 coronavirus disease or COVID-19) (Zhu et al., 2020).  
42 SARS-CoV-2 was declared pandemic by WHO on March 11, 2020.

43 Healthcare professionals who are involved in aerosol-generating procedures on  
44 COVID-19 patients are required to use FFP2-classified filter facepiece respirators for  
45 respiratory protection against SARS-CoV-2 infection. FFP2-respirators (from now on called  
46 ‘facemask’) filter at least 94% of the submicron-sized test aerosols with NaCl, according to  
47 the NEN-EN 149:2001 + A1:2009 standards (**Table 1**). These standards are used by the  
48 accredited test laboratories (the so-called notified bodies) within the European Union member  
49 states to test and certify the facemasks upon approval. According to these standards, FFP2-  
50 classified facemasks are also required to meet the criteria for inward leakage, maximal CO<sub>2</sub>-  
51 content of inhaled air, and breathing resistance, which are summarized in **Table 1**.

52 As the global demand for FFP2-facemasks largely exceeded the production,  
53 distribution and test capacities of the conventional suppliers and notified bodies during the  
54 COVID-19 pandemic, we formed a Dutch collaborative initiative, consisting of the Reinier de  
55 Graaf hospital, Royal DSM, Delft University of Technology, Leiden University Medical  
56 Center and Erasmus University Medical Center, with the aim to design and produce  
57 facemasks that meet the FFP2-specifications. Those locally-produced facemasks were initially  
58 tested with custom-made developed test equipment for a NaCl penetration test, fit test, and  
59 breathing resistance test under conditions that approximate the NEN-EN149 standards before  
60 being tested and approved by a certified test laboratory. Those setups have been described in  
61 detail in Blad et al., 2020 (submitted). The facemasks were also tested on virus filtration  
62 efficiency (VFE) with the mouse hepatitis virus (MHV), a beta coronavirus that causes lethal

63 hepatitis in mice (Gledhill et al., 1955), but that is non-pathogenic to humans. This test  
64 provides additional and biologically more relevant evidence for the filtration efficiency of  
65 submicron-sized particles by the facemask's filter material. These studies identified mask  
66 designs that protect against coronavirus-loaded aerosols with an efficiency similar to that of a  
67 commercial FFP2-facemask.

68

## 69 **METHODS**

70

71 *Facemask designs.* Three different types of in-house designed facemasks were tested  
72 in triplicate in various custom-made experimental setups. The “Reinier 0.1” facemask (**Fig.**  
73 **1a**) was constructed with a dental facemask, that consisted of two layers polypropylene  
74 nonwoven fabric (40 and 20 gr m<sup>-2</sup>) and a single layer of 20 g m<sup>-2</sup> melt-blown fabric, to which  
75 two extra layers of spun-bond polypropylene filters (100 and 20 g m<sup>-2</sup>) was added. The “DSM  
76 1.0” facemask (**Fig. 1b**) consisted of five polypropylene nonwoven filter layers that consisted  
77 of 55 g m<sup>-2</sup> spunmelt, 20 g m<sup>-2</sup> melt-blown, 30 g m<sup>-2</sup> melt-blown, 20 g m<sup>-2</sup> melt-blown, and 47  
78 g m<sup>-2</sup> spunmelt polypropylene filters. The name of this mask refers to the collaboration with  
79 the Dutch nutrition and health company Royal DSM during the development of this facemask.  
80 The “Reinier 1.0” facemask (**Fig. 1c**) consisted of three layers: two layers of spun-bond  
81 polypropylene filters (100 and 20 gr m<sup>-2</sup>) and a single 20 gr m<sup>-2</sup> melt-blown polypropylene  
82 layer. The facemasks were benchmarked against the FFP2-certified 3M Aura 1862(+)  
83 facemask.

84 *The dry particle penetration test.* The dry environmental particle penetration test was  
85 performed to provide an initial indication of the filtering capacity of the in-house designed  
86 facemasks. The experimental setup consisted of a Solair 3200 particle counter (Lighthouse)  
87 that was connected with a particle chamber, on which a facemask was fixed in an airtight  
88 manner. The particle counter generated a flow of 56.6 L min<sup>-1</sup>, which created an air velocity

89 of 0.25 m sec<sup>-1</sup> through the facemask's filter material. Particles in the range of 0.3 –  
90 0.5 µm, 0.5 – 5.0 µm, and 5.0 – 25.0 µm in size were counted. First, a reference count of the  
91 number of environmental particles (# particles<sub>Ref</sub>) was performed in absence of a facemask  
92 and subsequently, the number of environmental particles was counted after fixing a facemask  
93 on the particle chamber (# particles<sub>mask</sub>). For each of the three particle size ranges, the filter  
94 capacity was calculated according to the following formula:

95

$$96 \text{ Filter capacity (\%)} = ((\# \text{ particles}_{Ref} - \# \text{ particles}_{mask}) / \# \text{ particles}_{Ref}) \times 100$$

97

98 *NaCl particle penetration test.* For the NaCl particle penetration test a PVC-tube  
99 system was constructed with a 90° bend, going from a vertical to a horizontal direction (the  
100 design and instructions to build are online available at [https://projectmask.nl/testing/filter-](https://projectmask.nl/testing/filter-material-penetration/build/)  
101 [material-penetration/build/](https://projectmask.nl/testing/filter-material-penetration/build/)). The vertical part of the tube system was connected with an  
102 Atomizer Aerosol Generator ATM 226, and the distal end of the horizontal part contained a  
103 PMMA tube with a sample holder in which a facemask was fixed in an airtight manner (**Fig.**  
104 **S1**). The aerosol generator produced NaCl particles from a 2% NaCl solution. The number of  
105 NaCl particles that passed through the facemask's filter material was counted by a TSI  
106 PortaCount Pro 8030 particle counter, which generated an air velocity of 0.1 m sec<sup>-1</sup> through  
107 the filter material of the facemasks. The number of particles that passed through the filter  
108 material was analysed with TSI FitPro<sup>+</sup> software.

109 *The fittest.* The fittest was performed to determine the leakage of particles around the  
110 edges of the facemasks. First, a probe was placed in the facemask by which it was connected  
111 to the PortaCount particle counter. To obtain representative results, each facemask was tested  
112 by three different individuals, who performed eight different exercises: normal breathing,  
113 deep breathing, moving the head side to side, moving the head up and down, talking, grimace,

114 bending over and normal breathing, as described in the NEN-149 standards. The particle  
115 leakage was determined by comparing the number of particles in front and behind the  
116 facemask's filter material and was recorded with a PortaCount particle counter. The data were  
117 analysed with the TSI FitPro<sup>+</sup> software.

118 *The breathing resistance test.* The breathing resistance of the facemasks was  
119 determined with a custom-made experimental setup (**Fig. S2**; the design and instructions to  
120 build are online available at <https://projectmask.nl/testing/breathing-resistance/build/>). The  
121 facemask was placed on a manikin head (described in Zhuang and Bradtmiller et al., 2005)  
122 that was connected to a tube system, in which the pressure drop after the filter material was  
123 recorded. Before testing the facemasks, the pressure sensors were calibrated without any  
124 specimen at inlet or exit (open flow), blockage of the exit (blocked flow), or with a known  
125 flow resistance. When adding the masks, the increasing airspeed led to an increased airflow  
126 through the facemask and a pressure drop in the system, which was related to the resistance.

127 *Virus filtration efficiency test.* As no standardized test procedures exist to determine  
128 the virus filtration efficiency of facemasks, an in-house designed experimental setup was used  
129 that consisted of a curved tube with a 0.45 m vertical and a 0.9 m horizontal part with at the  
130 distal end a sample holder for airtight placement of a facemask (**Fig. S3**). This tube was  
131 connected to a mixing chamber, in which the virus-loaded aerosols were mixed with mist  
132 droplets, that was generated by an ultrasonic mist maker, for more efficient virus collection.  
133 The mixing chamber was connected to three SKC BioSampler impingers, in which the  
134 collected virus was impinged into 45 ml virus transport medium (VTM) (HMEM (Lonza),  
135 12% v/v glycerol, 0.5% w/v Lactalbumin enzymatic hydrolysate, 0.02 mg ml<sup>-1</sup> Polymyxin B  
136 sulfate, 0.01 mg ml<sup>-1</sup> Nystatin, Penicillin/Streptomycin mixture 240/240 U ml<sup>-1</sup> and 0.3 mg  
137 ml<sup>-1</sup>). The maximal airflow in each SKC BioSampler was 12.5 L min<sup>-1</sup>, generating a total  
138 maximal flow of 37.5 L min<sup>-1</sup>. The facemasks were challenged with mouse hepatitis virus

139 (MHV), a beta coronavirus that causes hepatitis in mice, to be able to perform these tests  
140 under laboratory biosafety level (BSL) 2 conditions.  $10^8$  plaque-forming units (PFUs) of  
141 MHV were aerosolized with an Aerogen Solo nebulizer, originally used to nebulize  
142 medication in hospital-settings, in the vertical part of the tube, directed through the 90 °  
143 bend, and subsequently the horizontal part of the tube system with the airtight fixed facemask.  
144 The facemasks were placed in the sample holder in an airtight manner between two sanitary  
145 rings with a diameter of 40 mm, which created an air velocity of  $0.42 \text{ m sec}^{-1}$  at a continuous  
146 airflow of  $31.5 \text{ L min}^{-1}$  ( $3 \times 12.5 \text{ L min}^{-1}$  minus  $6 \text{ L min}^{-1}$  for the mist maker). The self-made  
147 facemasks were tested in triplicate and benchmarked against the FFP2-certified 3M Aura  
148 1862(+) facemask. The aerosolized virus was also collected in the absence of a facemask as a  
149 reference. Between each test, the tube system was flushed with HEPA-filtered air for 15 min  
150 at a flow of  $37.5 \text{ L min}^{-1}$ .

151 *Virus quantification.* Viral RNA copy number was quantified by a quantitative  
152 reverse-transcription polymerase chain reaction (RT-qPCR) analyses and the number of  
153 infectious virus particles by plaque assays.

154 For RT-qPCR, viral RNA was isolated from  $135 \mu\text{l}$  VTM with the QIAamp Viral  
155 RNA Mini Kit (Qiagen) according to the manufacturer's protocol. Equine arteritis virus  
156 (EAV) was added to the lysis buffer as an internal control for the RNA isolation and RT-  
157 qPCR efficiency as described in Scheltinga *et al.*, 2005. The isolated RNA was converted to  
158 copy DNA (cDNA) and quantified in a TaqMan Fast Virus 1-step master mix (Applied  
159 Biosystems) in the presence of  $450 \text{ nM}$  primers (MHV-FPr1:  
160 ACGCCGCCTTATTAAGATG, MHV-RPr1: GGCATAGCACGATCACATTT) and  $200$   
161  $\text{nM}$  probe (TexRed-TCCTGTACTCATGGGTT GGGACTATCC-BHQ2) that targets the  
162 viral gene *nsp12*, coding for RNA dependent RNA polymerase (RdRp). The primers and  
163 probe for the EAV internal control were also added and have been described in Loens *et al.*,

164 2012. The reactions were run in a CFX384 Q-PCR Thermocycler (BioRad) with a two-step  
165 protocol: Cycle 1 (1x): 50 °C, 5 min. and 95 °C for 20 sec., and Cycle 2 (45x): 95 °C for 5 sec.  
166 and 60 °C for 30 sec. An MHV standard was generated by *in vitro* transcription with the T7  
167 mMessage mMachine kit (ThermoFisher) according to the manufacturer's protocol and was  
168 also analysed as described above to determine the copy number of viral RNA in the samples.

169 The number of infectious virus particles was determined by a plaque assay.  $8 \times 10^5$   
170 17CL1 cells, derived from mouse (*Mus musculus*) BALB/c fibroblasts, were seeded in six-  
171 wells plates and incubated overnight at 37°C. The cells were inoculated by incubation with an  
172 undiluted or one of the diluted MHV samples from a ten-fold serial dilution for 1 hr at 37°C.  
173 After inoculation, the cells were washed twice with PBS, overlaid with an Avicell (Sigma)  
174 overlay, and incubated for an additional 24 hrs at 37°C. The cells were subsequently fixated  
175 with 3.4% formaldehyde in PBS for 1 hr at room temperature and stained with 0.75% crystal  
176 violet staining solution for 5 min at room temperature. After removal of the staining solution,  
177 the wells were washed with water, and the number of plaques was counted.

178

## 179 **RESULTS AND DISCUSSION**

180 *NaCl particles were more efficiently filtered than the environmental particles.*

181 To obtain a first indication of the filtering capacities of the three types of locally-  
182 produced facemasks, the filtration of dry environmental particles in a size range of 0.3 – 25  
183 µm was determined using the Solair 3200 particle counter with and without airtight placement  
184 of one of the facemasks on the particle chamber. When the FFP2-certified facemask was  
185 placed on the particle chamber, 99.4±0.08% of the environmental particles of between 0.3-0.5  
186 µm were filtered, and 98.9±0.27% and 95.8±1.55% of the particles of respectively 0.5-5.0 and  
187 5.0-25.0 µm (**Fig. 2**). Varying results were obtained when the newly designed facemasks were  
188 tested in this setup. The Reinier 0.1-facemasks filtered 84±0.34% of the 0.3-0.5 µm particles,  
189 and 94.4±0.74% and 97.9±1.66% of 0.5-5.0 and 5.0-25.0 µm particles respectively. The DSM  
190 1.0-facemasks showed stable filtering performances and filtered around 98% of the

191 environmental particles in the three size ranges. The Reinier 1.0-facemasks on the other hand  
192 showed variable filtering performances. 0.3-0.5  $\mu\text{m}$  and 0.5-5.0  $\mu\text{m}$  particles were filtered for  
193 91.4 $\pm$ 0.25% and 96.6 $\pm$ 0.88% respectively, while particles of the 5.0-25.0  $\mu\text{m}$  size range were  
194 filtered for 94.5 $\pm$ 7.90%. The reason for the varying filtering performances in the last particle  
195 size range is unclear as the particles smaller than 5.0  $\mu\text{m}$  were filtered to a similar extent  
196 throughout the experiment. This dataset indicates that the Reinier 0.1-facemask was least  
197 capable of filtering particles of between 0.3-0.5  $\mu\text{m}$ , and that the DSM 1.0-facemask  
198 performed most similar to the FFP2-certified mask.

199 The particle filtration efficiencies of the three facemask designs were further tested  
200 under conditions that closely approximate the NEN-149 standards with aerosolized NaCl  
201 particles. According to these standards, FFP2-facemasks are required to filter at least 94% of  
202 the NaCl particles. In our experimental setup, the FFP2-certified facemask filtered  
203 98.13 $\pm$ 0.84% of the NaCl particles (**Fig 3**). The Reinier-0.1 and 1.0 facemasks filtered  
204 respectively 98.9 $\pm$ 0.42% and 99.3 $\pm$ 0.36% of the NaCl particles. This is significantly more  
205 than observed for environmental dry particles between 0.3 – 5.0  $\mu\text{m}$ , which was even below  
206 the FFP2 filtration threshold of 94% (**Fig. 2**). The Reinier-0.1 and -1.0 facemasks contained a  
207 single melt-blown polypropylene layer and the above-described observations indicate that the  
208 two layers nonwoven fabric of the three-layer dental facemask of the Reinier-0.1 model could  
209 be removed without affecting the facemask's filtering performance. The DSM 1.0-facemasks,  
210 the only type with three layers of melt-blown polypropylene filters, showed the highest NaCl-  
211 particle filtration efficiency of 99.83 $\pm$ 0.12% (**Fig. 3**). This model also performed best in the  
212 environmental particle filtration test (**Fig 2**).

213 The observed discrepancy between the two filtration tests could be explained by  
214 varying volumetric flows and air velocities between the different experiments, as it has also  
215 been shown by others that these factors affect the facemask's filtering performances



216 (Rengasamy et al., 2010, 2011, Gao et al., 2016, Mukhametzanov et al., 2016). The air  
217 velocity during the environmental particle penetration test was 2.5 times higher than during  
218 the filtration test of NaCl particles and stresses the importance of standardized conditions  
219 when assessing the filter capacity of facemasks. Currently, the filtration of NaCl particles is  
220 the golden standard when testing the facemask's filter capacity for its certification and is  
221 considered in the literature as most conservative (Rengasamy et al., 2017). The NaCl-particle  
222 filtration efficiency of the Reinier 0.1- and DSM 1.0-facemasks was also verified by notified  
223 bodies and showed similar filtration efficiencies as in this study (**Fig. S4 and S5.**), confirming  
224 that the custom-made setup indeed results in similar measurements as under the conditions of  
225 the NEN149 standards. Hence, a good indication has been obtained that the filter capacity of  
226 the three types of locally-produced facemasks meets the FFP2 requirement under standardized  
227 conditions.

228 ***The prototype facepiece facemasks filter at least 98% of virus-loaded aerosols.***

229 To provide biologically-relevant measurements regarding their protective ability  
230 against virus-loaded aerosols, the facemasks were challenged with MHV, a beta coronavirus  
231 that infects mice.  $10^8$  PFU of MHV was aerosolized, passed through a tube with and without  
232 airtight fixation of a facemask after which the air, that went through the filter material was  
233 sampled and analysed for the presence of the virus. The high number of PFUs was required to  
234 observe at least 2 logs decrease in the number of PFUs, equivalent to 99% filtration, as it was  
235 expected that most virus particles might be lost after nebulization into the tube system. The  
236 three types of facemask were tested in two separate sessions, which resulted in two  
237 independent datasets (**Fig. 4 and 5**) In the no mask-control, MHV was aerosolized into the  
238 tube system and sampled in absence of a facemask in the sample holder to determine the  
239 maximum amount of virus that could be recovered from the air. This resulted in virus  
240 recovery of  $4.09 \pm 0.21$  log PFU ml<sup>-1</sup> in the first -, and  $5.89 \pm 0.21$  log PFU ml<sup>-1</sup> in the second  
241 session (**Fig. 4a and 5a**), indicating that the virus collection efficiency in the latter session

242 was higher than in the first session. Nevertheless, the collection efficiency of infectious virus  
243 particles was high enough to be able to observe at least a 2-logs decrease in virus collection  
244 after placing a facemask in the sample holder. When an FFP2-certified facemask was placed  
245 in the sample holder, the amount of infectious virus and viral RNA copies that were recovered  
246 behind the facemask were respectively on average 2.3- and 2.4-logs lower than in the no-  
247 mask control in the first session. This corresponds to filtration efficiencies of 99.4 and 99.6%  
248 (**Fig. 4a and b**). When this type of facemask was used in the second session, the infectious  
249 virus and viral RNA recovery decreased by respectively 3.1- and 3.5-logs on average, which  
250 corresponds to 99.92 and 99.96% filtration efficiency (**Fig. 5a and b**). The Reinier 0.1-  
251 facemasks reduced the recovery of infectious virus and RNA copies on average by 2.1 and  
252 2.8-logs respectively compared to the no mask-control. This corresponds with the filtration  
253 efficiencies of 99.2 and 99.9% (**Fig. 4**). 2.3 and 2.6-log reductions were observed with the  
254 DSM 1.0-facemasks, which corresponds with 99.3 and 99.6% filtration efficiency. The  
255 Reinier 1.0-facemasks were tested in the second session, which reduced the infectious virus  
256 and total viral RNA copy numbers with 3.1- and 2.6 logs on average, corresponding to 99.92  
257 and 99.71% filter efficiency (**Fig. 5**).

258 The virus filtration efficiency of the locally-produced facemasks was determined at a  
259 continuous air velocity of  $0.42 \text{ m sec}^{-1}$ , which is significantly higher than during the above  
260 described NaCl particle penetration test. Similar particle filtration efficiencies were  
261 nevertheless observed in these two experiments. This air velocity is also higher than described  
262 in various other studies where the virus filtration efficiencies of facemasks were tested  
263 (Borkow et al., 2010, Harnish et al., 2013, 2016, Rengasamy et al., 2017, Zhou et al., 2018). It  
264 was chosen here to test at  $0.42 \text{ m sec}^{-1}$  as this is a more physiological relevant air velocity  
265 during inhalation as the maximal air velocity during an inhalation cycle reaches up to 1 m/sec  
266 (Tang et al., 2013). Although bacteriophages, influenza viruses, and rhinoviruses have

267 previously been used in filtration experiments (Borkow et al., 2010, Harnish et al., 2013,  
268 2016, Rengasamy et al., 2017, Zhou et al., 2018), here a coronavirus was used for the first  
269 time. Despite the higher air velocity and the usage of a different virus, at least 98% of the  
270 virus-loaded aerosols were filtered by the FFP2-certified facemask, similarly as observed in  
271 the prementioned studies. The locally-produced facemasks showed similar virus filtration  
272 efficiencies as the FFP2-certified facemask, which suggests that these are equally protective  
273 against coronavirus-loaded aerosols.

274 ***Reinier-0.1 and -1.0 facemasks have acceptable inward leakage around the edges.***

275 In addition to the filtering capacity of the facemask's filter material, a proper fit is also  
276 crucial for the protective quality of the facemask (Rengasamy et al., 2011, Serfoze et al.,  
277 2017). It had been modeled by others that when the area of inward leakage at the facemask's  
278 edges exceeds 0.1% of its total surface area, the facemask is unable to offer 95% protection  
279 (Mukhametzanov et al., 2016). Therefore the three locally-produced facemasks were fit-tested  
280 to estimate their protective quality when used by individuals. Those individuals performed  
281 various exercises while wearing the facemask as described in material and methods. FFP2-  
282 certified facemasks are allowed to have an average inward leakage of maximal 8 or 11%,  
283 depending on the number of tests and exercises (**Table 1**). As our facemasks were tested by  
284 only three different persons, not the average, but maximal observed inwards leakage was  
285 taken as a measure for the fit of a facemask (**Table 2**), thus defining a worst-case scenario.  
286 The FFP2-certified facemasks showed a maximal inward leakage of 0.5% (**Table 2**). The  
287 Reinier 1.0-facemasks showed the best fit of the self-designed masks with a maximal  
288 observed inward leakage of 0.8%, whereas the DSM 1.0-facemasks showed a maximal inward  
289 leakage of 14.6%. The Reinier 0.1-facemasks showed a maximal inward leakage of 4.8%.  
290 These observations indicate that based on three study subjects, the Reinier-0.1 and -1.0  
291 models have acceptable fits.

292 ***The locally-produced facemasks can be safely used, regarding breathing resistance.***

293 The breathing resistance of the facemasks was determined to obtain an indication  
294 about the wearer's comfort and safety when wearing these facemasks. Therefore, the  
295 facemasks were placed on a manikin head and the pressure drop was recorded while the  
296 airflow was increased. The maximal pressure drop at an inhalation flow of 30 or 95 L min<sup>-1</sup>  
297 according to the NEN-149 standards is 0.7 and 2.4 mbar respectively. The pressure drops  
298 varied between 0.14 and 0.16 mbar at a continuous flow of 30 L min<sup>-1</sup>, and at a flow of 95 L  
299 min<sup>-1</sup>, the pressure drop varied between 0.74 and 0.85 mbar for all three facemask models  
300 (**Table 3**). Exhalation at a continuous flow of 160 L min<sup>-1</sup> resulted in a pressure drop of  
301 between 1.11 and 1.44 mbar for the three different designs, which is below the 3.0 mbar that  
302 is allowed according to the NEN-149 standards. These observations indicate that all three  
303 designs meet the NEN149 standards regarding breathing resistance. However, for the DSM-  
304 facemask this result might be due to the significant amount of inward leakage.

305

## 306 **CONCLUSION**

307

308 It is concluded that the Reinier 0.1 and -1.0 facemasks provide good respiratory  
309 protection against coronavirus-loaded aerosols and with similar efficiency as a certified FFP2  
310 mask, suggesting that these can be safely used by healthcare professionals.

311

## 312 **ACKNOWLEDGMENTS**

313

314 This work was supported by the NIH/NIAID (contract number HHSN272201400008C) and  
315 European Union's Horizon 2020 research and innovation program VetBioNet (grant  
316 agreement No 731014). Part of this research was supported by the Leiden University Fund  
317 (LUF), the Bontius Foundation, and donations from the crowdfunding initiative "wake up to  
318 corona". S.H. was funded in part by an NWO VIDI grant (contact number 91715372). Part of  
319 this research was supported by ZonMw initiative "creative solutions against CoVID-19"

320 (5001-0013). The authors also wish to thank Monique Elsing-van Olphen for supporting this

321 research and for supplying information on the facemask designs.

322

323

324 **REFERENCES**

325

326 Borkow, G., Zhou, S. S., Page, T., & Gabbay, J. (2010). A novel anti-influenza copper oxide  
327 containing respiratory face mask. *PLoS One*, *5*.

328 Gao, S., Kim, J., Yermakov, M., Elmashae, Y., He, X., Reponen, T., & Grinshpun, S. A.  
329 (2016). Performance of N95 FFRs against combustion and NaCl aerosols in dry and  
330 moderately humid air: Manikin-based study. *Ann. Occup. Hyg.*, *60*, 748-760.

331 Gledhill, A. W., Dick, G. W. A., & Niven, J. S. (1955). Mouse hepatitis virus and its  
332 pathogenic action. *J. Pathol. Bacteriol.*, *69*, 299-309.

333 Harnish, D. A., Heimbuch, B. K., Husband, M., Lumley, A. E., Kinney, K., Shaffer, R. E., &  
334 Wander, J. D. (2013). Challenge of N95 filtering facepiece respirators with viable H1N1  
335 influenza aerosols. *Infect. Control Hosp. Epidemiol.*, *34*, 494-499.

336 Harnish, D. A., Heimbuch, B. K., Balzli, C., Choe, M., Lumley, A. E., Shaffer, R. E., &  
337 Wander, J. D. (2016). Capture of 0.1- $\mu\text{m}$  aerosol particles containing viable H1N1 influenza  
338 virus by N95 filtering facepiece respirators. *J. Occup. Environ. Hyg.*, *13*, D46-D49.

339 Loens, K., Van Loon, A. M., Coenjaerts, F., Van Aarle, Y., Goossens, H., Wallace, P., &  
340 Leven, M. (2012). Performance of different mono-and multiplex nucleic acid amplification  
341 tests on a multipathogen external quality assessment panel. *J. Clin. Microbiol.*, *50*, 977-987.

342 Mukhametzanov, I. T., Grinshpun, S. A., Zaripov, S. K., & Gilfanov, A. K. (2016). Assessing  
343 the protection provided by facepiece filtering respirator: New model involving spherical  
344 porous layer with annular peripheral opening. *Aerosol Air Qual. Res.*, *16*, 2428-2437.

345 NEN -EN 149:2001+A1 :2009. Respiratory protective devices -Filtering half masks to protect  
346 against particles - Requirements, testing, marking. 2009

- 347 Rengasamy, S., Eimer, B., & Shaffer, R. E. (2010). Simple respiratory protection—evaluation  
348 of the filtration performance of cloth masks and common fabric materials against 20–1000 nm  
349 size particles. *Ann. Occup. Hyg.*, *54*, 789-798.
- 350 Rengasamy, S., & Eimer, B. C. (2011). Total inward leakage of nanoparticles through  
351 filtering facepiece respirators. *Ann. Occup. Hyg.*, *55*, 253-263.
- 352 Rengasamy, S., Shaffer, R., Williams, B., & Smit, S. (2017). A comparison of facemask and  
353 respirator filtration test methods. *J. Occup. Environ. Hyg.*, *14*, 92-103.
- 354 Scheltinga, S. A., Templeton, K. E., Beersma, M. F. C., & Claas, E. C. J. (2005). Diagnosis of  
355 human metapneumovirus and rhinovirus in patients with respiratory tract infections by an  
356 internally controlled multiplex real-time RNA PCR. *J. Clin. Virol.*, *33*, 306-311.
- 357 Serfozo, N., Ondráček, J., Otáhal, P., Lazaridis, M., & Ždímal, V. (2017). Manikin-based  
358 size-resolved penetrations of CE-marked filtering facepiece respirators. *J. Occup. Environ.*  
359 *Hyg.*, *14*, 965-974.
- 360 Tang, J. W., Nicolle, A. D., Klettner, C. A., Pantelic, J., Wang, L., Suhaimi, A. B., ... &  
361 Cheong, D. D. (2013). Airflow dynamics of human jets: sneezing and breathing-potential  
362 sources of infectious aerosols. *PLoS One*, *8*.
- 363 World Health Organization. (2020). *Rational use of personal protective equipment for*  
364 *coronavirus disease (COVID-19) and considerations during severe shortages: interim*  
365 *guidance, 6 April 2020* (No. WHO/2019-nCov/IPC\_PPE\_use/2020.3). World Health  
366 Organization.
- 367 Zhou, S. S., Lukula, S., Chiossone, C., Nims, R. W., Suchmann, D. B., & Ijaz, M. K. (2018).  
368 Assessment of a respiratory face mask for capturing air pollutants and pathogens including  
369 human influenza and rhinoviruses. *J. Thorac. Dis.*, *10*, 2059.

370 Zhu, N., Zhang, D., Wang, W., Li, X., Yang, B., Song, J., & Niu, P. (2020). A novel  
371 coronavirus from patients with pneumonia in China, 2019. *N. Engl. J. Med.*

372 Zhuang, Z., & Bradtmiller, B. (2005). Head-and-face anthropometric survey of US respirator  
373 users. *J. Occup. Environ. Hyg.*, 2, 567-576.

374



**Table 1:** Requirements for FFP2-classified FFRs according to the NEN-EN149 standards

<b>Filter penetration test</b>	<b>FIT-test</b>	<b>CO<sub>2</sub> content test</b>	<b>Breathing resistance test</b>	
Max. penetration of 120 mg NaCl test aerosol at 95 L min <sup>-1</sup>	Max. inward leakage	Max. CO <sub>2</sub> content of inhaled air	Inhalation	Exhalation
6%	8 <sup>a</sup> or 11 <sup>b</sup> %	<1% on average	0.7 mbar at 30 L min <sup>-1</sup> 2.4 mbar at 95 L min <sup>-1</sup>	3.0 mbar at 160 L min <sup>-1</sup>

<sup>a</sup> for at least 8/10 individual wearer arithmetic means

<sup>b</sup> for at least 46/50 individual exercise results (e.g. 10 subjects x 5 exercises)

375

376

377

**Table 2:** Maximal and minimal observed inward leakage

<b>Facemask</b>	<b>Max. observed inward leakage (%)</b>	<b>Min. observed inward leakage (%)</b>
<b>3M Aura 1862+ (FFP2)</b>	0.5	0.5
<b>Reinier 0.1</b>	4.8	4.2
<b>DSM 1.0</b>	14.6	6.7
<b>Reinier 1.0</b>	0.8	0.5

378

379

**Table 3:** Pressure drop over the self-designed facemasks at continuous inhalation flows of 30 or 95 L min<sup>-1</sup> and an exhalation flow of 160 L min<sup>-1</sup>.

<b>Facemask</b>	<b>Inhalation 30 L min<sup>-1</sup> (0.7 mbar max.)</b>	<b>Inhalation 95 L min<sup>-1</sup> (2.4 mbar max.)</b>	<b>Exhalation 160 L min<sup>-1</sup> (3.0 mbar max.)</b>
<b>Reinier 0.1</b>	0.14 ± 0.003	0.74 ± 0.009	1.44 ± 0.05
<b>DSM 1.0</b>	0.14 ± 0.003	0.84 ± 0.008	1.31 ± 0.06
<b>Reinier 1.0</b>	0.16 ± 0.002	0.85 ± 0.01	1.11 ± 0.06

380

381

382 **Figure captions**

383 **Fig. 1.** The designs of the three locally-produced facemasks with Reinier-0.1 (a), DSM-1.0  
384 (b), and Reinier-1.0 (c).

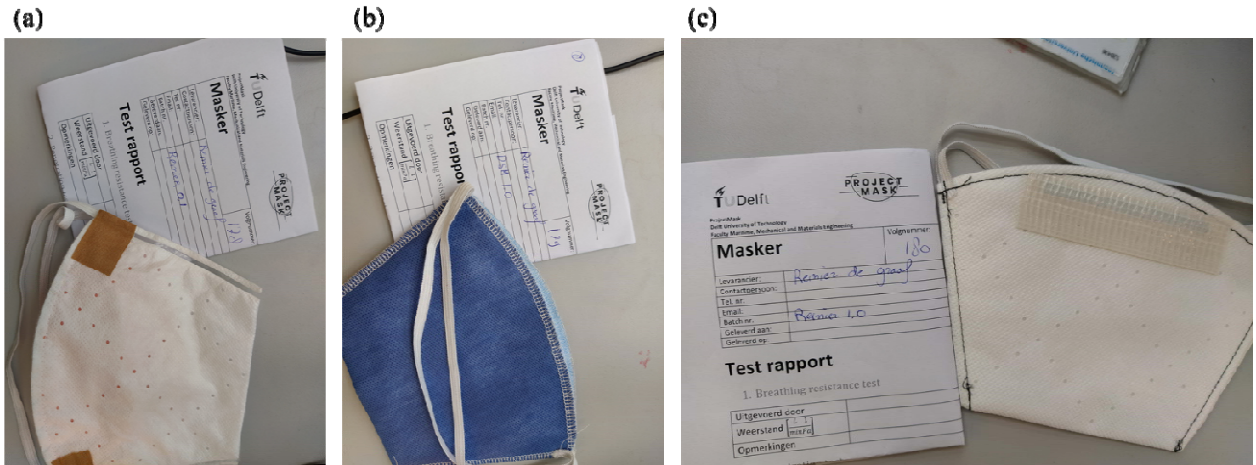
385 **Fig. 2.** Filtration efficiency of environmental dry particles by the locally-produced facemasks  
386 and benchmarked against an FFP2-certified facemask.

387 **Fig. 3.** Filtration of NaCl-particles by the self-designed facemasks close to the NEN-149  
388 standard conditions.

389 **Fig. 4.** Physical and biological collection of aerosolized mouse hepatitis virus (a) and  
390 filtration efficiencies (b) observed for facemask Reinier 0.1 or DSM 1.0.

391 **Fig. 5.** Physical and biological collection of aerosolized mouse hepatitis virus (a) and  
392 filtration efficiencies (b) observed for facemask Reinier 1.0

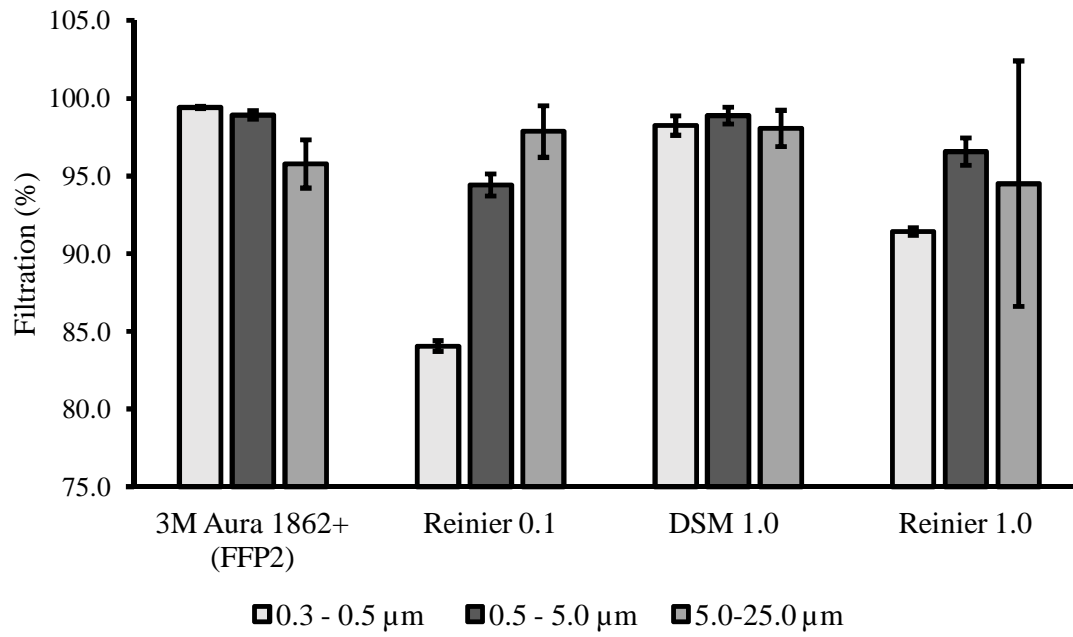
393



394

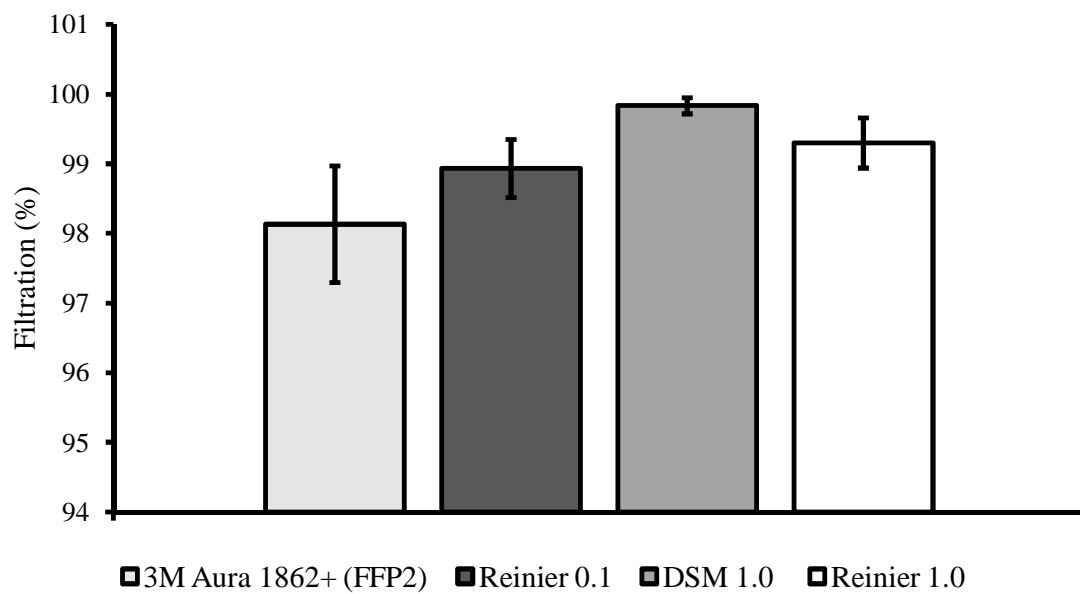
395 **Fig. 1.**

396



397

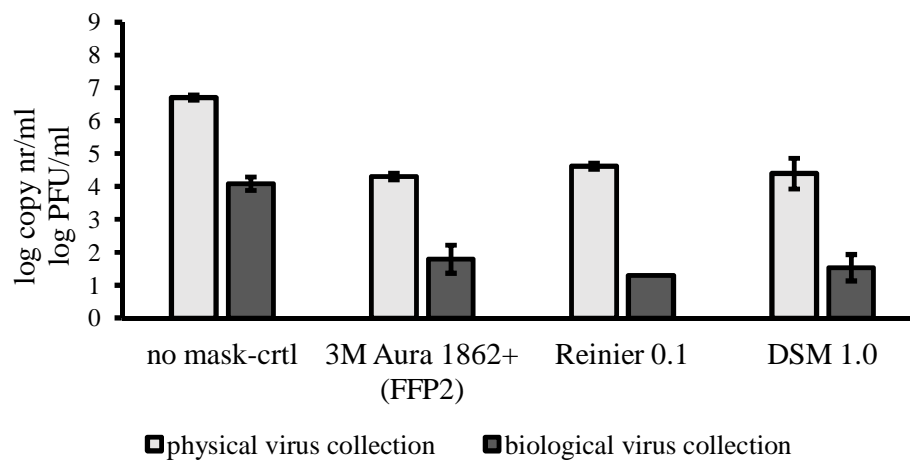
398 **Fig. 2.**



399

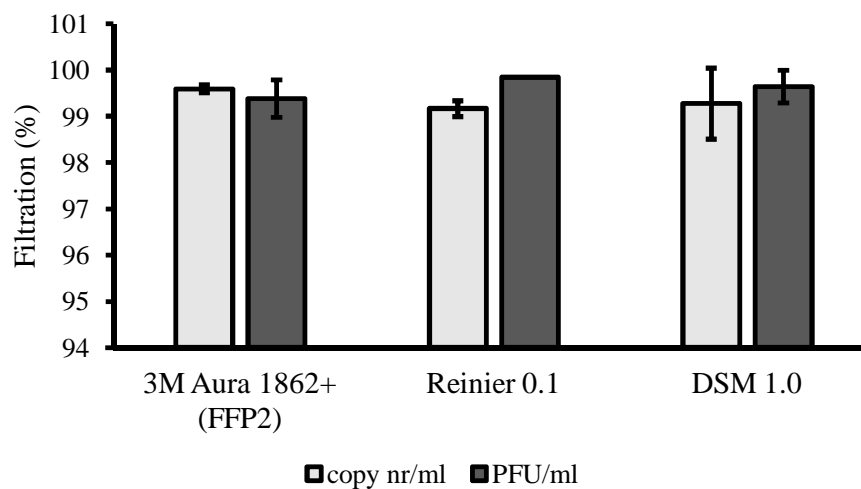
400 **Fig. 3.**

401 (a)



402

403 (b)



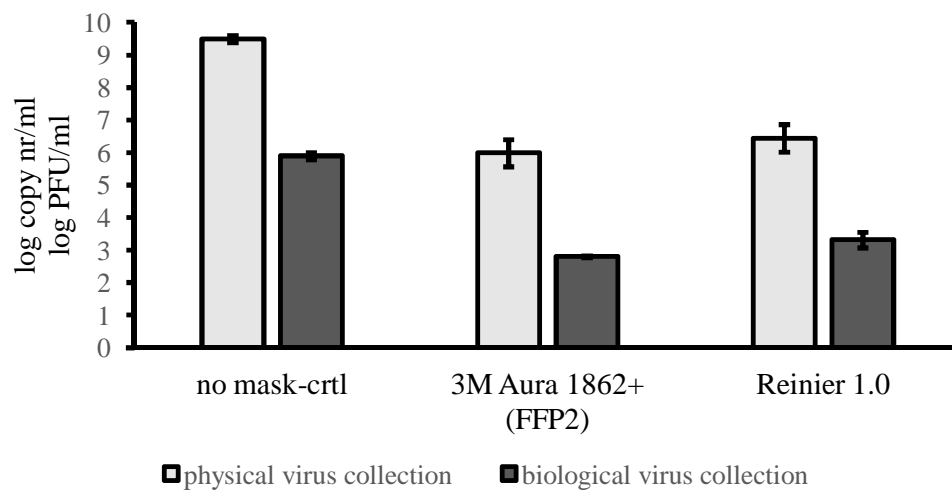
404

405 **Fig. 4.**

406

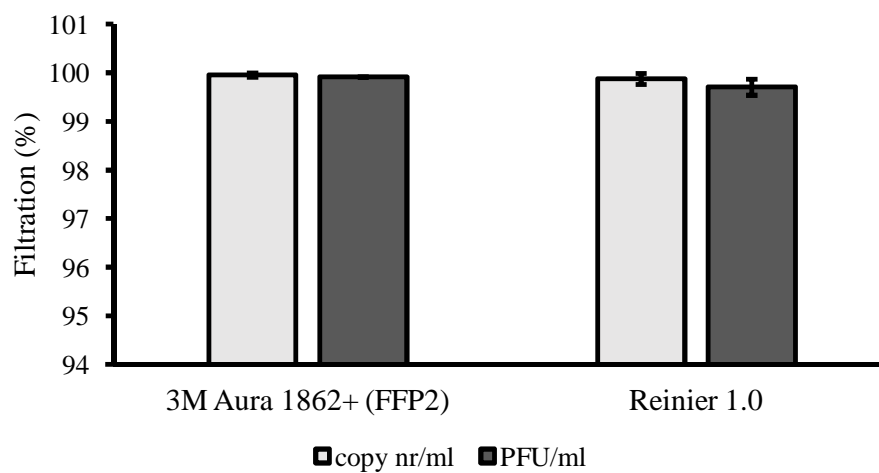


407 (a)



408

409 (b)



410

411 **Fig. 5.**

412

413

414

415

